

A New Marine Cyrtophorid Ciliate, *Dysteria nabia* nov. spec. (Ciliophora: Phyllopharyngea: Cyrtophorida: Dysteriidae), from South Korea

Mi-Hyun PARK and Gi-Sik MIN

Department of Biological Sciences, Inha University, Incheon, South Korea

Abstract. We discovered a new marine cyrtophorid ciliate, *Dysteria nabia* nov. spec., in Incheon Harbor in the Yellow Sea and at Ihotou Beach on Jeju-do Island, South Korea. This new species is described based on live observations, protargol impregnation, and silver nitrate impregnation. *Dysteria nabia* measures approximately $94 \times 45 \mu\text{m}$ *in vivo* and has an oval to elliptical form, with a subcaudally positioned podite; 5 right kineties, with a single shortened innermost right kinety; usually 3 left frontal kineties; and 2 contractile vacuoles. The length of the small subunit ribosomal RNA (SSU rRNA) gene sequence is 1,700 bp. In comparison with the five previously identified sequences of *Dysteria* species, the inter-specific similarity of *D. nabia* ranges from 91.5 to 98.4%.

Key words: Dysteriidae, *Dysteria nabia* nov. spec., infraciliature, marine ciliate, SSU rRNA, Korea, Yellow Sea.

INTRODUCTION

Most species of *Dysteria* (Ciliophora: Phyllopharyngea: Cyrtophorida: Dysteriidae) are morphologically specialized benthic ciliates occurring in marine habitats. Only a few species are found in fresh waters (Kahl 1931). *Dysteria* species are characterized by bilaterally flattened body shape, oral structure with conspicuous cytopharynx, and restricted ciliature in the anterior and ventral regions (Kahl 1931, Deroux 1965, Dragesco 1966, Wilbert 1971, Song and Wilbert 2002, Chen *et al.* 2011). The somatic ciliature of *Dysteria* species is

comprised of several right ventral kineties, a single short equatorial fragment, left equatorial kineties, several oral kineties, and a single terminal fragment. The right ventral kineties usually differ in length, with two or more rows extending to the apical groove, and are composed of numerous basal body pairs. Recent studies performed using silver impregnation have revealed that the ciliature is highly species specific, particularly with respect to the number and general pattern of the somatic ciliature in the right field (Petz *et al.* 1995; Song and Packroff 1997; Song and Wilbert 2002; Wilbert and Song 2005; Gong *et al.* 2007; Chen *et al.* 2011; Pan *et al.* 2011). Gong *et al.* (2007) constructed a key of 16 marine species, based on morphology and infraciliature with the number of right kineties being one of the main characters in identifying *Dysteria* species.

Address for correspondence: Gi-Sik Min, Department of Biological Sciences, Inha University, 100 Inharo, Nam-gu, Incheon 402-751, South Korea, Tel: +82-32-860-7692; Fax: +82-32-874-6737; E-mail: mingisik@inha.ac.kr

To date, more than 30 *Dysteria* morphospecies have been investigated, among which 19 have been re-described or newly described using modern methods, i.e., protargol and silver nitrate impregnation (Fauré-Fremiet 1965; Petz *et al.* 1995; Gong *et al.* 2002, 2003, 2007; Song and Wilbert 2002; Gong and Song 2003, 2004; Hu and Suzuki 2005; Wilbert and Song 2005; Chen *et al.* 2011; Pan *et al.* 2011). During the last decade, 17 of the 19 species have been reported in China and Japan. In the present study, we report for the first time the occurrence of *Dysteria* species in the coastal waters of Korea. We present a morphological description of the new species, *Dysteria nabia*, and distinguish the species based on sequence comparison of small subunit ribosomal RNA (SSU rRNA).

MATERIALS AND METHODS

Sample collection, observation, and identification

We discovered *Dysteria nabia* nov. spec. on January 13, 2011 in Incheon Harbor (37°26'N, 126°35'E; salinity, 30.6 psu; temperature, -0.6°C) in the Yellow Sea, and on October 3, 2011 at Ihotu Beach (33°30'N, 126°28'E; salinity, 18.3–23.4 psu) on Jeju-do Island, South Korea.

The ciliates were collected by filtering the washed seawaters of mussels and seaweeds that were sampled around the beaches and harbors, and incubated in Petri dishes at room temperature. Bacteria in the cultures were enriched by adding rice grains. The specimens were observed by using bright-field and differential interference contrast microscopy, at magnifications of $\times 50$ to $\times 1,000$. The protocol method of Foissner (1991) was used to reveal the infraciliature. The Chatton-Lwoff method was used to reveal the silverline systems (Corliss 1953). Counts and measurement of stained specimens were performed at a magnification of $\times 1,000$ (Leica DM2500; Wetzlar, Germany). Terminology follows that of Corliss (1979), Gong and Song (2004), and Chen *et al.* (2011).

DNA extraction, amplification, and sequencing

A single living specimen from each population was isolated under a dissecting microscope (Olympus SZX12, Tokyo, Japan), washed 5 times in sterilized seawater of the appropriate salinity, and then transferred to 1.5-mL microcentrifuge tubes. Genomic DNA extraction was carried out using a RED Extract-N-Amp™ Tissue PCR Kit (Sigma-Aldrich, St. Louis, MO, USA). Amplification of the SSU rRNA gene was performed according to Jung *et al.* (2011). Sequencing of the purified PCR products was carried out using the following two internal primers designed in this study: Cyr18S580F, 5'-AGT TAA AAA GCT CGT AGT TG-3'; and Cyr18S920F, 5'-AGA ACG AAA GTT AGG GGA TC-3'. Sequencing was carried out using an ABI PRISM® 3700 DNA Analyzer (Applied Biosystems, Foster City, CA, USA) with a Dye Terminator Cycle Sequencing Ready Reaction Kit (Applied Biosystems, Foster City, CA, USA).

Phylogenetic analysis

Two SSU rRNA sequences of *D. nabia* were determined by direct sequencing of the PCR products. The six SSU rDNA sequences of the family Dysteriidae, and six of the family Hartmannulidae were retrieved from the GenBank database. The *Chlamydodon obliquus* was used as an outgroup. Sequence alignment was carried out using Clustal X 1.81 computer program (Jeanmougin *et al.* 1998). Sequence variations among the species were calculated using MEGA4 software (Tamura *et al.* 2007), with the Kimura 2-parameter.

For the phylogenetic analysis, we selected GTR + I (0.4320) + G (0.7640) under the Akaike information criterion (AIC), the best model suggested by the jModelTest 2.1.1 program (Darriba *et al.* 2012). We used PhyML 3.0 (Guindon and Gascuel 2003) to construct a maximum likelihood (ML) tree. The reliability of internal branches was assessed using the non-parametric bootstrap method with 1,000 replicates. Bayesian inference (BI) using MrBayes 3.1.2 (Ronquist and Huelsenbeck 2003) was performed with the Markov chain Monte Carlo algorithm. The program was run for 1,000,000 generations, with a burn-in of 300,000.

RESULTS AND DISCUSSION

Dysteria nabia nov. spec. (Figs 1A–F, 2A–I, 3A–J; Table 1)

Diagnosis. Marine *Dysteria*, size approximately $94 \times 45 \mu\text{m}$ *in vivo*; body oval to elliptical in outline; with five right kineties, the outermost two of which extend dorso-apically; the innermost right kinety conspicuous shortened; macronucleus about $33 \times 15 \mu\text{m}$ *in vivo*; two ventral contractile vacuoles.

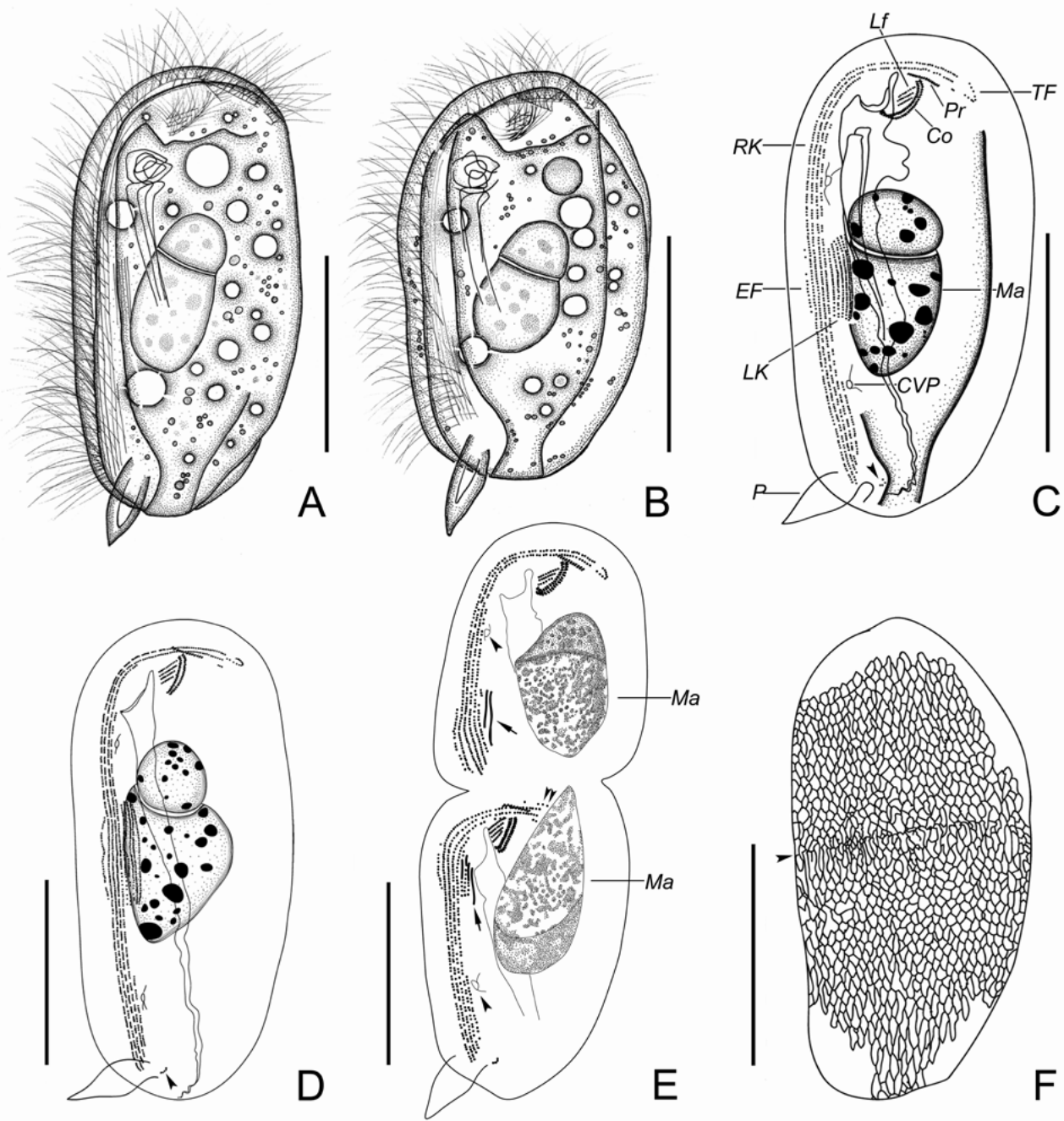
Type locality. Marine waters with mussels and seaweeds, Incheon Harbor (37°26'N, 126°35'E), the Yellow Sea, South Korea.

Other localities. Coastal waters, Ihotu Beach (33°30'N, 126°28'E), Jeju-do Island, Korea strait, South Korea.

Type specimens. Two hapantotype slides (one with protargol-impregnated specimens, NIBRPR000104270; one with silver nitrate-impregnated specimens, NIBRPR0000104271) and two paratype slides (NIBRPR0000104272–NIBRPR0000104273) of protargol-impregnated specimens were deposited in the National Institute of Biological Resources, South Korea.

Etymology. The name originates from the Korean word “nabi” (meaning butterfly), indicating that this organism moves like the sitting form of a butterfly folding its wings.

Description. Cell size $74\text{--}113 \times 42\text{--}49 \mu\text{m}$ *in vivo*, on average $94 \times 45 \mu\text{m}$, body bilaterally flattened. Body outline usually oval to elliptical, ventral and dorsal



Figs 1A–F. Morphology of *Dysteria nabia* nov. spec. from life (A, B), after protargol (C–E), and silver nitrate impregnation (F). The hapantotype (A–E) and paratype (F) specimens were investigated. **A, B** – left side view of two individuals with differing body size and shape; **C, D** – left side view showing the infraciliature, arrowheads indicate the kinetosome-like granules at the base of the podite; **E** – left side view of late-stage divider, showing the anlagen for the left kineties (arrows), the contractile vacuole pores (arrowheads), and the anlagen for terminal fragments in the opisthe (double-headed arrow); **F** – left side view showing the silverline system, arrowhead indicates the equatorial transverse stripe. Co – circumoral kineties, CVP – contractile vacuole pore, EF – equatorial fragment, Lf – left frontal kineties, LK – left kineties, Ma – macronucleus, P – podite, Pr – preoral kineties, RK – right kineties, TF – terminal fragment. Scale bars: 40 μ m.

Table 1. Morphometric characteristics of *Dysteria nabia* nov. spec. based on protargol-impregnated specimens (all measurements in μm).

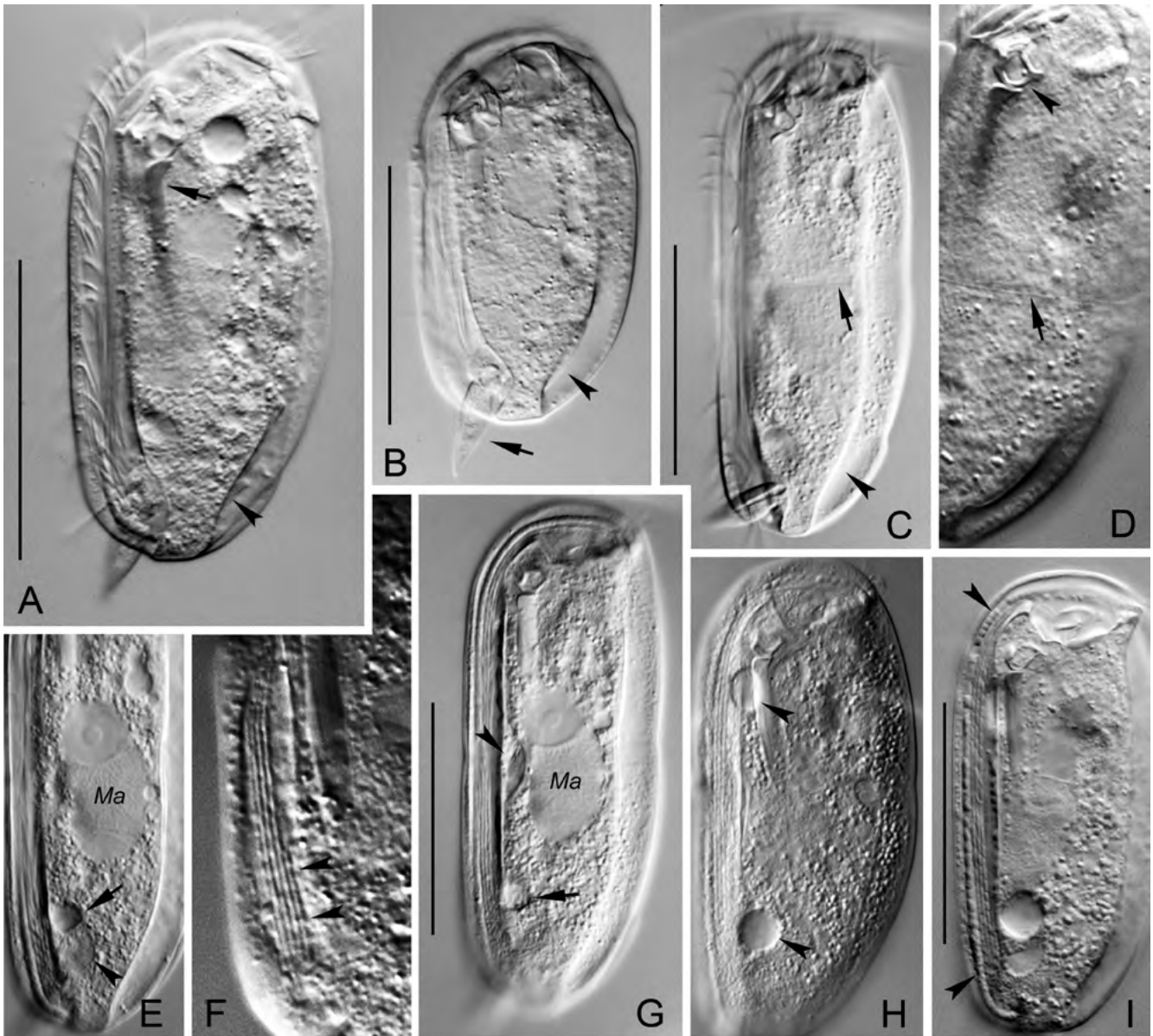
	Min	Max	Mean	SD	SE	CV	n
Body, length	79.0	113.0	99.3	10.6	2.1	10.6	26
Body, width	38.0	49.0	45.0	3.2	0.6	7.2	26
Right kineties, number	5.0	5.0	5.0	0.0	0.0	0.0	26
Frontoventral kineties, number	2.0	2.0	2.0	0.0	0.0	0.0	25
Left equatorial kineties, number	5.0	7.0	6.3	0.8	0.2	12.0	24
Kinetosomes in outermost right kinety, number	163.0	208.0	187.5	15.8	5.6	8.5	8
Kinetosomes in innermost right kinety, number	18.0	28.0	22.5	3.1	0.9	13.7	13
Kinetosomes in terminal fragment, number	6.0	10.0	9.1	1.2	0.3	13.0	16
Kinetosomes in equatorial fragment, number	10.0	33.0	16.7	8.1	2.4	48.4	11
Macronucleus, length	35.0	47.0	41.6	3.6	0.7	8.6	24
Macronucleus, width	16.0	25.0	20.6	2.6	0.5	12.7	24
Glandule, diameter	6.0	12.0	8.3	1.5	0.3	18.0	23
Kinetosome-like granule, number	4.0	6.0	5.0	0.5	0.2	10.7	8
Left frontal kineties, number	3.0	4.0	3.1	0.3	0.1	8.8	3
Podite, length	15.0	19.0	16.6	1.2	0.2	7.1	25

CV – coefficient of variation in %; Max – maximum; Mean – arithmetic mean; Min – minimum; n – number of individuals examined; SD – standard deviation; SE – standard error of the mean.

sides almost parallel. In dividing cells, body form rectangular in outline. Anterior margin blunt, posterior region blunt or round. When observed from ventral view, left plate concave and right plate convex. Right plate slightly wider than left plate (Figs 1A, B, 2A–C). Under high magnification, one equatorial transverse strip positioned approximately at equatorial region on surface of both plates (Figs 2C, D, 3B). Podite large and dagger-shaped, approximately 18 μm in length *in vivo*, subcaudally located on left ventral side (Figs 1A–E, 2A–C). Glandule located near the base of podite, approximately 8 μm in diameter (Fig. 2E; Table 1). Cilia restricted to ventral and apical grooves between left and right plates, approximately 12 μm long *in vivo*. Five right kineties even discernible *in vivo* (Figs 1C, D, 2F, 3A). Cytoplasm colorless to grayish and light-brown, containing several food vacuoles, approximately 3–11 μm in diameter, and numerous small granules spread over the body (Figs 1A, B, 2A–I). Cytostome in anterior 1/6–1/7 of body, located ventrally. Cytopharynx con-

spicuous *in vivo*, longitudinally oriented and extending to posterior end of cell, supported by 2 relatively strong nematodesmal rods, tipped with one complex tooth (Figs 1C, D, 3D). Two ventral contractile vacuoles, approximately 8 μm in diameter *in vivo*, one in anterior 1/3–1/4 of body, the other in posterior 1/3–1/4 of body (Figs 1A–D, 2H, 3A, G). Macronucleus elongate and large, approximately 33 \times 15 μm *in vivo*, positioned in body center, characteristically heteromerous, with the posterior part more hyaline than the anterior (Figs 1A–D, 2E, G, 3A). Micronucleus not detected. Locomotion by slowly and wobbly crawling.

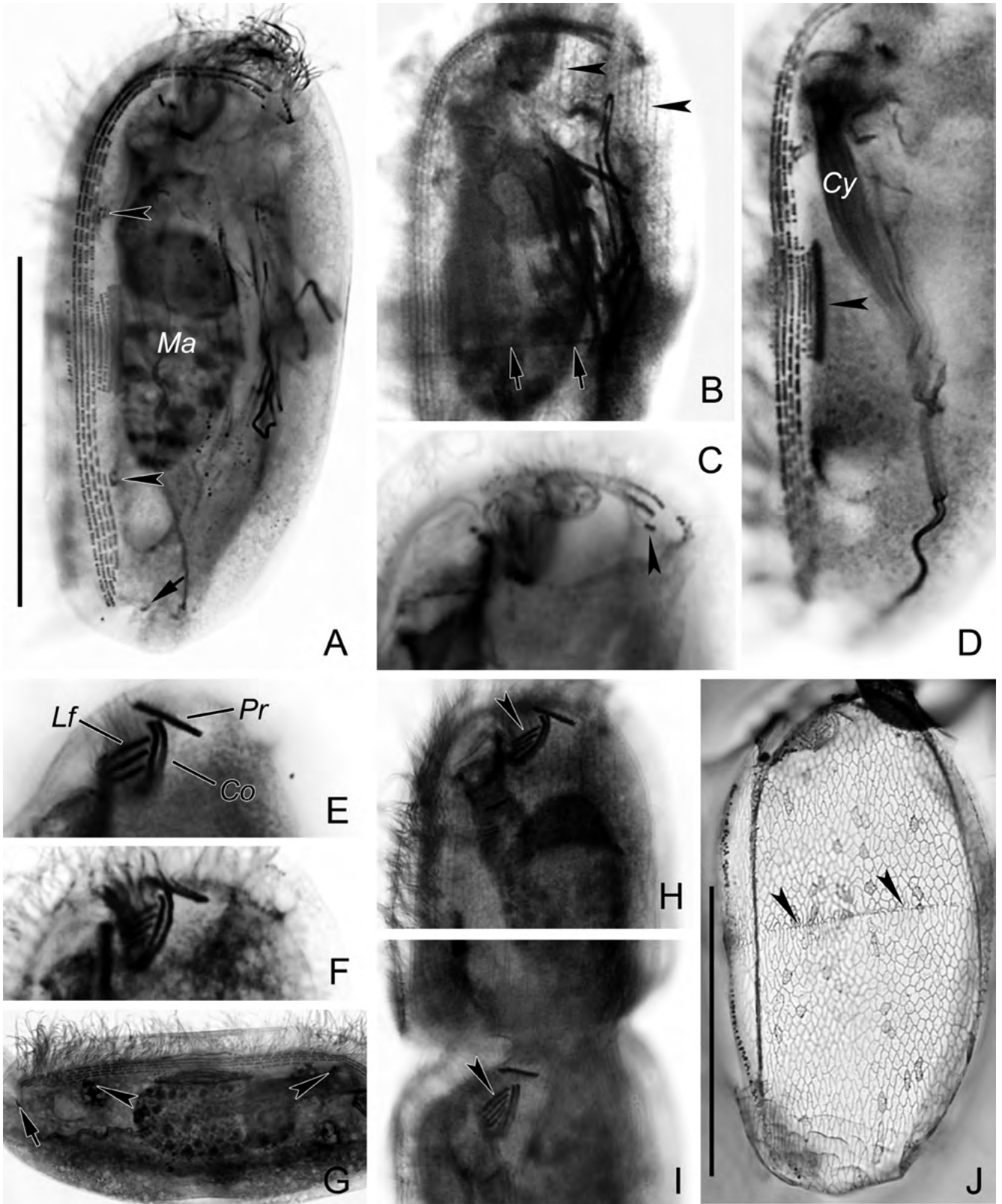
Infraciliature as shown in Figs 1C, D, 2F, 3A, C–I. Five right kineties, with the innermost row conspicuously shortened. Two outermost right kineties approximately equal in length, extending anteriorly to dorsal margin; the outermost kinety consisting of approximately 188 basal bodies (mookinetes), comprising of 2–6 (average 4) basal body pairs (monokinety pairs). A single innermost right kinety, with 18–28 basal bod-



Figs 2A–I. Photomicrographs of living specimens of *Dysteria nabia* nov. spec. **A, B** – left lateral view of two typical individuals, arrows in (A) and (B) indicate the cytopharyngeal rod and podite, respectively, arrowheads indicate the groove on the left plate; **C** – left lateral view of an elongate specimen, arrow indicates the equatorial transverse stripe and arrowhead the groove on the left plate; **D** – left side view, arrow indicates the equatorial transverse stripe and arrowhead the complex teeth; **E** – left side view, arrow indicates the contractile vacuole pore and arrowhead the glandule; **F** – right kineties of the posterior portion, arrowheads indicate the innermost right kinety; **G** – left side view, arrow indicates the contractile vacuole pore and arrowhead the left kineties; **H–I** – left side view, arrowheads in (H) and (I) indicate the contractile vacuole pore and protuberances on the margins of the right kineties, respectively. Ma – macronucleus. Scale bars: 50 μ m.

ies, located in posterior 1/3–1/4 of body (Figs 1C, D, 2F). The remaining two right kineties gradually shortened from right to left (Figs 1C, D, 2F, 3A). Five to seven left kineties, densely arranged close to right kineties, and positioned around equator (Figs 1C, D, 3A, D). Terminal fragment antero-dorsally located, and

forming hook-like shape comprising 6–10 basal bodies. Equatorial fragment composed of 10–33 basal bodies (Table 1). Two to three basal body pairs antero-dorsally located under two outermost right kineties (Figs 1C, D, 3C). Four to six kinetosome-like granules positioned near base of podite (Figs 1C–E, 3A, G).



Arrangement of kineties in oral field typical of the genus: 2 parallel circumoral kineties slightly curved to left; preoral kinety obliquely positioned in anterior region; usually 3 left frontal kineties, located on right of circumoral kineties. Circumoral kineties and preoral kinety consisting of dikinetids, and parallel left kineties composed of monokinetids (Figs 1C–E, 3E, F, H–I). After protargol impregnation, several straight stripes were detected on surface of plates (Fig. 3B).

Comparison. To date, 19 nominal *Dysteria* species have been investigated using silver impregnation methods. Among these, 12 species were referred to by Gong and Song (2004). The new species can be distinguished from other *Dysteria* species by its oval to elliptical body shape, body size, five right kineties with a single shortened innermost row, and macronucleus size.

Dysteria nabia closely resembles *D. ovalis* (Gourret and Roeser, 1886) Kahl, 1931, *D. pectinata* (Nowlin, 1913) Kahl, 1931, *D. procera* Kahl, 1931, and *D. proraefrons* Clark, 1865 in terms of cell size, body shape, cytopharynx length, shortened innermost row of right kineties, and marine habitat. However, *D. nabia* differs from *D. pectinata* in several features, namely, its slightly larger body size ($74\text{--}113 \times 42\text{--}49 \mu\text{m}$ vs. $60\text{--}100 \times 30\text{--}55 \mu\text{m}$) and oval to elliptical body shape, with ventral and dorsal sides almost parallel (vs. body semi-oval in outline, with ventral side straight and dorsal convex). In addition, *D. nabia* has a groove on the posterior left lateral side from life (vs. no groove), fewer right kineties (5 vs. 7), and a larger number of basal bodies in the equatorial fragment ($10\text{--}33$ vs. $3\text{--}27$) (Table 2; Figs 4B, E–F; Gong *et al.* 2007). *Dysteria procera* is similar in body size to *D. nabia* ($80\text{--}110 \times 25\text{--}40 \mu\text{m}$ vs. $74\text{--}113 \times 42\text{--}49 \mu\text{m}$), but has fewer right kineties (3 vs. 5) and fewer basal bodies in the equatorial fragment ($3\text{--}15$ vs. $10\text{--}33$), and a smaller macronucleus ($24\text{--}36 \times 8\text{--}12 \mu\text{m}$ vs. $35\text{--}47 \times 16\text{--}25 \mu\text{m}$) (Table 2; Figs 4G, H; Gong and

Song 2003). *Dysteria proraefrons* can also be distinguished from *D. nabia* by its slightly smaller body size ($60\text{--}90 \times 30\text{--}50 \mu\text{m}$ vs. $74\text{--}113 \times 42\text{--}49 \mu\text{m}$), a larger number of right kineties (6 vs. 5), smaller number of basal bodies in the equatorial fragment ($2\text{--}11$ vs. $10\text{--}33$), and smaller macronucleus ($20\text{--}45 \times 6\text{--}15 \mu\text{m}$ vs. $35\text{--}47 \times 16\text{--}25 \mu\text{m}$) (Table 2; Figs 4I, J; Pan *et al.* 2011). *Dysteria ovalis* has 4 right kineties (vs. 5 in *D. nabia*) and a different pattern of oral kineties (Table 2; Figs 4B, C; Fauré-Fremiet 1965).

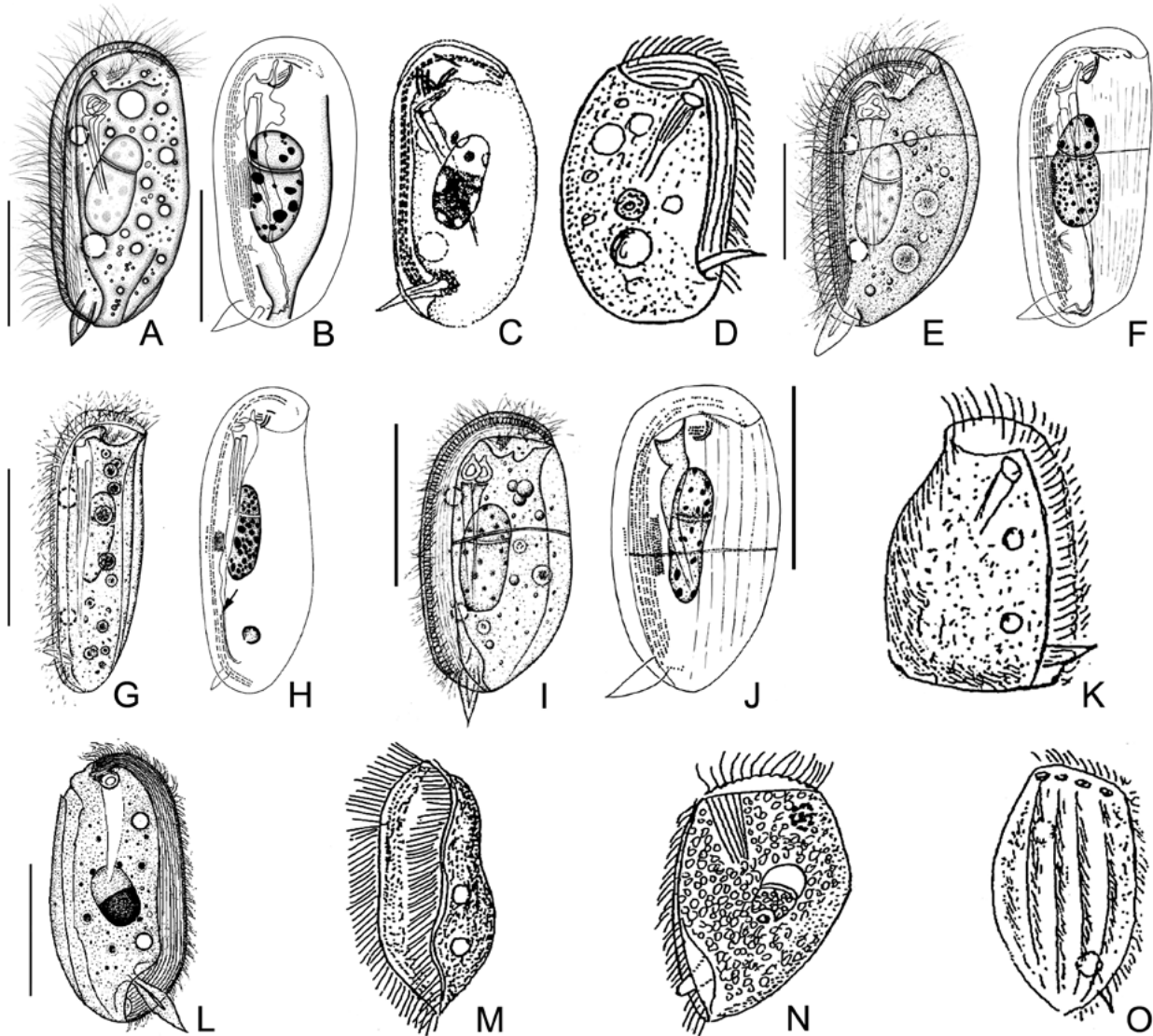
Dysteria monostyla (Ehrenberg 1838) Kahl, 1931, *D. brasiliensis* Faria *et al.*, 1922, *D. calkinsi* Kahl, 1931, and *D. antarctica* Gong *et al.*, 2002 have the same number of right kineties as *D. nabia*. However, unlike *D. nabia*, these four species do not have a shortened innermost right kinety (Table 2; Figs 1C, D; Petz *et al.* 1995; Song and Packroff 1997; Gong *et al.* 2002, 2007; Song and Willbert 2002).

Dysteria armata Huxley, 1957, *D. crassipes* Claparède and Lachmann, 1859, and *D. lanceolata* Claparède and Lachmann, 1859 have similar body size with *D. nabia*. However, *D. armata* has 6 right kineties (vs. 5) with 4 dorso-apically extended right kineties (vs. 2) (Table 2; Figs 1C, D; Fauré-Fremiet 1965). *D. crassipes* has fewer number of right kineties (4 vs. 5), smaller macronucleus ($16\text{--}25 \times 8\text{--}14 \mu\text{m}$ vs. $35\text{--}47 \times 16\text{--}25 \mu\text{m}$), and numerous ectosymbiotic bacteria on surface of plate (vs. absent) (Table 2; Figs 1C, D; Gong *et al.* 2007). *D. lanceolata* has different body shape (nearly oval or approximately rectangular vs. oval or ellipsoid), larger number of right kineties (6–7 vs. 5), and 2 or 3 of dorso-apically extended right kineties (vs. always 2) (Table 2; Figs 1A–D, 2A–C; Chen *et al.* 2011).

Dysteria nabia must also be compared with some of 17 earlier described species that have not been described by using modern methods. In the present study, we compared *D. nabia* with two closely related species

◀

Figs 3A–J. Photomicrographs of *Dysteria nabia* nov. spec. after protargol impregnation (A–I) and after silver nitrate impregnation (J). **A** – left lateral view, arrow indicates the kinetosome-like granules and arrowheads indicate the contractile vacuole pore; **B** – left side view, arrows indicate the equatorial transverse stripe and arrowheads the fine stripes; **C** – left view of the anterior portion, arrowhead indicates the short row near the anterior end of the frontoventral kineties; **D** – cytopharynx, arrowhead indicates the left kineties; **E**, **F** – anterior portion, showing details of the oral ciliature; **G** – left side view, arrow indicates the kinetosome-like granules and arrowheads the contractile vacuole pore; **H**, **I** – oral ciliature on the left side of the late divider, arrowheads in (H) and (I) indicate the left frontal kineties in the proter and opisthe, respectively; **J** – left lateral view showing the silverline system, arrowheads indicate the equatorial transverse stripe. Co – circumoral kineties, Cy – cytopharynx, Lf – left frontal kineties, Ma – macronucleus, Pr – preoral kineties. Scale bars: 50 μm .



Figs 4A–O. Morphology and infraciliature of *Dysteria nabia* nov. spec. and closely related *Dysteria* species. **A, B** – *D. nabia* nov. spec. from life (**A**) and after protargol impregnation (**B**); **C–D** – *D. ovalis* (Gouret and Roeser, 1886) Kahl, 1931 (**C**, from Fauré-Fremiet 1965; **D**, from Kahl 1931); **E–F** – *D. pectinata* (Nowlin, 1913) Kahl, 1931 (from Gong *et al.* 2007); **G–H** – *D. procera* Kahl, 1931 (from Gong and Song 2003); **I–J** – *D. proraefrons* Clark, 1865 (from Pan *et al.* 2011); **K** – *D. angustata* (Claparede & Lachmann, 1858) (from Kahl 1931); **L** – *D. meridionalis* Dragesco, 1965 (from Dragesco 1966); **M** – *D. astyla* (Maskell, 1877) (from Kahl 1931); **N** – *D. reesi* Kahl, 1931 (from Kahl 1931); **O** – *D. sulcata* Claparede & Lachmann, 1858 (from Kahl 1931). Scale bars: 40 μm (**A–B**, **I–J**), 30 μm (**E**), 50 μm (**G**, **L**).

that resemble the new species in terms of body size, number of contractile vacuoles, and absence of a dorsal spine. *Dysteria meridionalis* Dragesco, 1965 and *D. astyla* (Maskell, 1877) are very similar to *D. nabia*. *Dysteria meridionalis* closely resembles *D. nabia* in terms of length *in vivo* (96 μm vs. 74–113 μm) and the presence of two contractile vacuoles; however, it has 12 (vs. 5) right kineties (Table 3; Figs 4B, L; Dragesco

1966). *Dysteria astyla* is similar to *D. nabia* in terms of shape (oval vs. oval to elliptical) and the presence of two ventral contractile vacuoles; however, it has a smaller body (70 \times 17.5 μm vs. 74–113 \times 42–49 μm) and occurs in a different habitat (freshwater vs. marine). *Dysteria astyla* has no podite, whereas *D. nabia* has a conspicuous podite, approximately 18 μm long *in vivo* (Table 3; Figs 4A, B, M; Kahl 1931).

Table 2. Comparison of *Dysteria nabia* with its 19 congeners investigated using modern methods.

Species	Body size <i>in vivo</i> (µm)	Body outline	Number of RKS	Number of dorso-apically extended RKS	Number of Lfs	Number of basal bodies in TF	Number of basal bodies in EF	Ma size after Impregnation (µm)	Data source
<i>Dysteria nabia</i>	74–113 × 42–49	oval to elliptical	5 ^b	2	3–4	6–10 (usually 10)	10–33	35–47 × 16–25	Original
<i>D. ovalis</i>	–	rectangular	4 ^{b,d}	2 ^d	3 ^d	–	–	–	Kahl (1931), Fauré-Fremiet (1965)
<i>D. pectinata</i>	60–100 × 30–55	semi-oval	7 ^b	2	3	6–9	3–27	30–43 × 12–18	Gong <i>et al.</i> (2007)
<i>D. procera</i>	80–110 × 25–40	elongate and slender	3 ^b	2	3	6–10	3–15	24–36 × 8–12	Gong and Song (2003)
<i>D. proraefrons</i>	60–90 × 30–50	oval	6 ^b	2	3	5–8	2–11	20–45 × 6–15	Pan <i>et al.</i> (2011)
<i>D. antarctica</i>	ca. 145 × 65	elongate, slender	5	3 ^c	3	ca. 15	–	38.5–41 × 21	Petz <i>et al.</i> (1995) Gong <i>et al.</i> (2002)
<i>D. brasiliensis</i>	120–140 × 46–60 ^a 55–80 × 35–40 ^a ca. 140 × 56 ^a	roughly triangular or elongate, with caudal spine ^a	5	2	3	–	–	32–50 × 12–21	Song and Packroff (1997) Gong <i>et al.</i> (2007)
<i>D. calkinsi</i>	30–50 × 20–25	slender, with 2 furrows	5	2 ^c	2 ^d	7 ^d	6 ^d	ca. 25 × 15	Song and Wilbert (2002)
<i>D. monosyla</i>	60–110 × 30–40	rectangular, elongate	5	2	3	7–10	10–23	18–32 × 8–18	Gong <i>et al.</i> (2002)
<i>D. armata</i>	80–120 × –	oval	6	4	3 ^d	–	–	–	Kahl (1931), Fauré-Fremiet (1965)
<i>D. crassipes</i>	50–80 × 30–50	nearly rectangular to pentagonal	4	2	3	7–10	9–34	16–25 × 8–14	Gong <i>et al.</i> (2007)
<i>D. cristata</i>	40–50 × 25–30	asymmetrically oval	3	2	3	3–5	3–9	9–16 × 5–7	Gong <i>et al.</i> (2002)
<i>D. derouxii</i>	75–110 × 30–50	rectangular	8–9	3	3	10–19	6–27	30–49 × 11–17	Gong and Song (2004), Pan <i>et al.</i> (2011)
<i>D. lanceolata</i>	60–80 × 30–60	nearly oval or approxi- mately rectangular	6–7	2–3	3	6–8	6–27	23–32 × 15–24	Chen <i>et al.</i> (2011)
<i>D. legumen</i>	40–60 × 25–35	oval to rectangular	6	2	2	5–8	2–14	15–25 × 8–13	Pan <i>et al.</i> (2011)
<i>D. magna</i>	150–160 × 100	broadly rectangular	8	2	3	ca. 40	15–47	ca. 50 × 30	Gong and Song (2003)
<i>D. parovalis</i>	50–80 × 40–60	broadly oval	9	3	2 ^d	–	ca. 10	28–40 × 13–17	Wilbert and Song (2005)
<i>D. pusilla</i>	15–30 × 10–20	rectangular	3	2	–	2	ca. 5	10–19 × 2.5–4	Gong <i>et al.</i> (2003)
<i>D. semilunaris</i>	20–40 × 12–20	nearly oval	4	2	3	2–5	2–9	11–20 × 4–8	Gong <i>et al.</i> (2007)
<i>D. yagiui</i>	140–200 × 60–100	elongate-rectangular	13	6	3	26–32	8–24	40–99 × 13–26	Hu and Suzuki (2005)

EF – equatorial fragment; Lfs – left frontal kineties; Ma – macronucleus; RKS – right kineties; TF – terminal fragment.

– Data not available.

^aSize showing tree types, data from Gong *et al.* (2007).^bWith innermost shortened right kinety.^cData from Gong and Song (2004).^dCount from illustration.

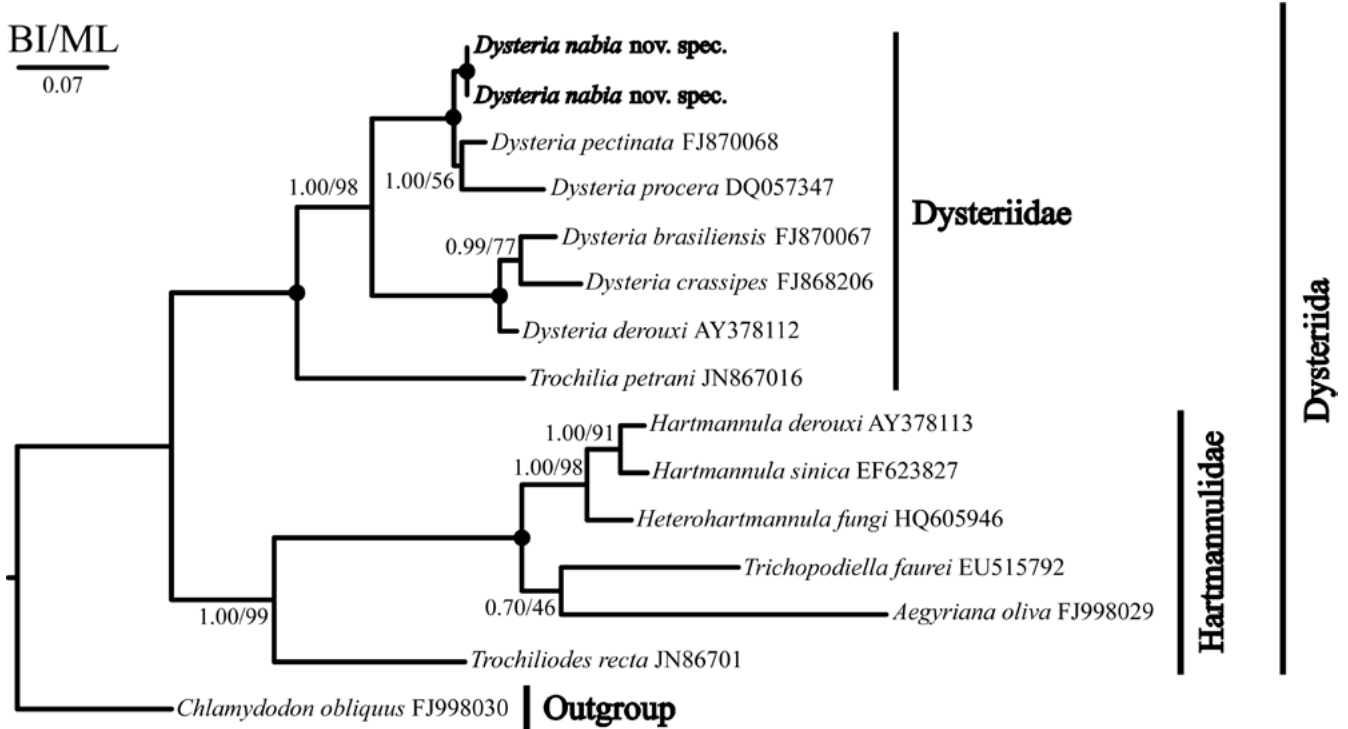


Fig. 5. Maximum likelihood tree based on SSU RNA gene sequences, showing the position of *Dysteria nabia* nov. spec. (bold font). Numbers at the nodes represent the Bayesian posterior probability value and the bootstrap values from maximum likelihood. Solid circles represent full support in both algorithms.

Table 3. Comparison of *Dysteria nabia* with 5 morphologically similar species of which the infraciliature remains unknown.

Species	Body size <i>in vivo</i> (µm)	Body outline	Dorsal spine	Podite position	Number of CV	Habitat	Data source
<i>Dysteria nabia</i>	74–113 × 42–49	oval to elliptical	absent	subcaudally	2	marine	This publication
<i>D. angustata</i>	–	anterior margin narrowed	absent	subcaudally ^b	2	marine	Kahl (1931)
<i>D. astyla</i>	70 × 17.5	oval	absent	not observed	2	freshwater	Kahl (1931)
<i>D. meridionalis</i>	96 × –	rectangular	absent	caudally	2	marine	Dragesco (1966)
<i>D. reesi</i>	59–68 × –	approx. oval	absent	in posterior 1/4 of body ^b	–	marine	Kahl (1931) Chen <i>et al.</i> (2011)
<i>D. sulcata</i>	150 × –	– ^a	absent	subcaudally ^b	–	marine	Kahl (1931)

CV – contractile vacuole.

– Data not available.

^aWith four ribs on the right plate.

^bData from illustration.

We further compared *D. nabia* with three other earlier described species, namely, *Dysteria angustata* (Claparède and Lachmann, 1858), *D. reesi* Kahl, 1931, and *D. sulcata* (Claparede and Lachmann, 1858). The

body size and infraciliature for *D. angustata* are not available, however, this species can be distinguished from *D. nabia* by its narrow, neck-like anterior margin whereas the ventral and dorsal sides of the anterior

margin in *D. nabia* are parallel (Table 3; Figs 4A, B, K; Kahl 1931). *Dysteria sulcata* differs from *D. nabia* in its larger body size (150 μm vs. 74–113 \times 42–49 μm) and presence of 4 ribs on the right plate (vs. no ribs) (Table 3; Fig. 4O; Kahl 1931). *Dysteria reesi* differs from *D. nabia* in its smaller body size (59–68 μm vs. 74–113 \times 42–49 μm), conspicuous pigment spot in the left anterior end (vs. no spot), and location of the podite (posterior 1/4 of body vs. subcaudally) (Table 3; Figs 2A–C, 4A, B, N; Kahl 1931).

Molecular investigation and analysis. The SSU rDNA sequences of two populations of *D. nabia* are identical, with a length of 1,700 bp. The sequence was deposited in GenBank under accession numbers KF725634 and KF725635. The sequence similarity between *D. nabia* and other *Dysteria* species ranged from 91.5% (*D. crassipes*) to 98.4% (*D. pectinata*). Despite the low inter-specific similarity, with 91.5%, it is slightly higher than other inter-specific similarity among four *Vorticella* spp., periphytic ciliates in the Peritrichs, ranging from 90.2 to 98.8%, identified by Gong *et al.* (2013). In the phylogenetic analysis, the family Dysteriidae was divided into two groups; however, the monophyly of this family was well supported, with high support values in the BI and ML analyses. *Dysteria nabia* formed a group with *D. procera* (96.4% in similarity) and *D. pectinata* (98.4%), while the remaining *Dysteria* species clustered as a second group (Fig. 5). Results of our molecular analysis based on sequence divergence and the phylogenetic tree supports the designation of *D. nabia* nov. spec. as a distinct and novel ciliate belonging to the genus *Dysteria*.

Acknowledgments. This work was supported by the grants of Inha University and the program on Management of Marine Organisms causing Ecological Disturbance and Harmful Effects funded by KIMST/MOF.

REFERENCES

- Chen X., Gong J., Al-Rasheid K. A. S., Farraj S. A., Song W. (2011) New contribution to the morphological taxonomy of three marine cyrtophorid ciliates from the Yellow Sea, China (Ciliophora: Cyrtophorida). *Acta Protozool.* **50**: 105–119
- Corliss J. O. (1953) Silver impregnation of ciliated protozoa by the Chatton-Lwoff technic. *Stain Technol.* **28**: 97–100
- Corliss J. O. (1979) The ciliated protozoa. Characterization, classification and guide to the literature. 2nd edn. Pergamon Press, Oxford
- Darriba D., Taboada G. L., Doallo R., Posada D. (2012) jModel-Test 2: more models, new heuristics and parallel computing. *Nat. Methods* **9**: 772
- Deroux G. (1965) Origine des cinéties antérieures, gauches et buccales dans le genre *Dysteria* Huxley. *Comptes Rendus de l'Académie des Sciences, Paris* **260**: 6689–6691
- Dragesco J. (1966) Observation sur quelques Cilies libres. *Arch. Protistenkd.* **109**: 155–206
- Fauré-Fremiet E. (1965) Morphologie des Dysteriidae (Ciliata Cyrtophorina). *Compt. Rend. Acad. Sci. Paris* **260**: 6679–6684
- Foissner W. (1991) Basic light and scanning electron microscopic methods for taxonomic studies of ciliated protozoa. *Eur. J. Protistol.* **27**: 313–330
- Gong J., Dong J., Liu X., Massana R. (2013) Extremely high copy numbers and polymorphisms of the rDNA operon estimated from single cell analysis of oligotrich and peritrich ciliates. *Protist* **164**: 369–379
- Gong J., Lin X. F., Song W. (2003) Redescription of a poorly-known marine cyrtophorid ciliate, *Dysteria pusilla* (Claparède et Lachmann, 1859) (Protozoa: Ciliophora: Cyrtophorida) from Qingdao, China. *Acta Protozool.* **42**: 215–221
- Gong J., Song W. (2003) Morphology and infraciliature of two marine benthic ciliates, *Dysteria procera* Kahl, 1931 and *Dysteria magna* nov. spec. (Protozoa, Ciliophora, Cyrtophorida), from China. *Eur. J. Protistol.* **39**: 301–309
- Gong J., Song W. (2004) Description of a new marine cyrtophorid ciliate, *Dysteria derouxi* nov. spec., with an updated key to 12 well-investigated *Dysteria* species (Ciliophora, Cyrtophorida). *Eur. J. Protistol.* **40**: 13–19
- Gong J., Song W., Warren A. (2002) Redescriptions of two marine cyrtophorid ciliates, *Dysteria cristata* (Gourret and Roeser, 1888) Kahl, 1931 and *Dysteria monostyla* (Ehrenberg, 1838) Kahl, 1931 (Protozoa, Ciliophora, Cyrtophorida), from China. *Eur. J. Protistol.* **38**: 213–222
- Gong J., Song W., Warren A., Lin X., Roberts D. M. (2007) Microscopical observations on four marine *Dysteria* species (Ciliophora, Cyrtophorida). *Eur. J. Protistol.* **43**: 147–161
- Guindon S., Gascuel O. (2003) A simple, fast, and accurate algorithm to estimate large phylogenies by maximum likelihood. *Syst. Biol.* **52**: 696–704
- Hu X., Suzuki T. (2005) Light microscopical observations on two marine dysteriid ciliates from Japan, including a description of *Dysteria yagiui* nov. spec. (Ciliophora, Cyrtophorida). *Eur. J. Protistol.* **41**: 29–36
- Jeanmougin F., Thompson J. D., Gouy M., Higgins D. G., Gibson T. J. (1998) Multiple sequence alignment with Clustal X. *Trends Biochem. Sci.* **23**: 403–405
- Jung J.-H., Baek Y.-S., Kim S., Choi H.-G., Min G.-S. (2011) A new marine ciliate, *Metaurostylopsis antarctica* nov. spec. (Ciliophora, Urostylelida) from the Antarctic Ocean. *Acta Protozool.* **50**: 289–300
- Kahl A. (1931) Urtiere oder Protozoa I: Wimpertiere oder Ciliata (Infusoria) 2. Holotricha außer den im 1. Teil behandelten Prostomata. *Tierwelt Dtl.* **21**: 181–398
- Pan H., Hu X., Gong J., Lin X., Al-Rasheid K. A. S., Al-Farraj S. A., Warren A. (2011) Morphological redescrptions of four marine ciliates (Ciliophora: Cyrtophorida: Dysteriidae) from Qingdao, China. *Eur. J. Protistol.* **47**: 197–207
- Petz W., Song W., Wilbert N. (1995) Taxonomy and ecology of the ciliate fauna (Protozoa, Ciliophora) in the endopagial and pelagial of the Weddell Sea, Antarctica. *Stapfia* **40**: 1–223
- Ronquist F., Huelsenbeck J. P. (2003) MrBayes 3: Bayesian phylogenetic inference under mixed models. *Bioinformatics* **19**: 1572–1574

- Song W., Packroff G. (1997) Taxonomy and morphology of marine ciliates from China with description of two new species, *Strombidium globosaneum* nov. spec. and *S. platum* nov. spec. (Protozoa, Ciliophora). *Arch. Protistenkd.* **147**: 331–360
- Song W., Wilbert N. (2002) Faunistic studies on marine ciliates from the Antarctic benthic area, including descriptions of one epizoic form, 6 new species, and 2 new genera (Protozoa: Ciliophora). *Acta Protozool.* **41**: 23–61
- Tamura K., Dudley J., Nei M., Kumar S. (2007) MEGA4: Molecular Evolutionary Genetics Analysis (MEGA) software version 4.0. *Mol. Biol. Evol.* **24**: 1596–1599
- Wilbert N. (1971) Morphologie und Ökologie einiger neuer Ciliaten (Holotricha, Cyrtophorina) des Aufwuchses. *Protistologica* **7**: 357–363
- Wilbert N., Song W. (2005) New contributions to the marine benthic ciliates from the Antarctic area, including description of seven new species (Protozoa, Ciliophora). *J. Nat. Hist.* **39**: 935–973

Received on 24th July, 2013; revised on 16th October, 2013; accepted on 10th January, 2014